https://doi.org/10.5194/egusphere-2023-2782
Preprint. Discussion started: 24 November 2023

Simulated terrestrial runoff shifts the metabolic balance of a coastal Mediterranean plankton community toward heterotrophy

Tanguy Soulié[1], Francesca Vidussi[1], Justine Courboulès[1], Marie Heydon[1], Sébastien Mas[2], Florian Voron[2], Carolina Cantoni[3], Fabien Joux[4], Behzad Mostajir[1]

[1]MARBEC (MARine Biodiversity, Exploitation and Conservation), Univ Montpellier, CNRS, Ifremer, IRD, Montpellier, France
[2]MEDIMEER (MEDIterranean Platform for Marine Ecosystems Experimental Research), OSU OREME, CNRS, Univ Montpellier, IRD, INRAE, Sète, France
[3]CNR-ISMAR (Istituto di Scienze Marine), Area Science Park, Basovizza, Ed. Q2, Trieste, Italy
[4]Sorbonne Université, CNRS, Laboratoire d'Océanographie Microbienne (LOMIC), Observatoire Océanologique de Banyuls, Banyuls/Mer, France

Correspondence to: Tanguy Soulié (tanguy.soulie@gmail.com), Behzad Mostajir (behzad.mostajir@umontpellier.fr)

Abstract. Climate change is projected to increase the frequency and intensity of extreme rainfall events in the Mediterranean region, increasing runoffs of terrestrial matter into coastal waters. To evaluate the consequences of terrestrial runoff on plankton key processes, an in situ mesocosm experiment was conducted for 18 days in the spring of 2021 in the coastal Mediterranean Thau Lagoon. Terrestrial runoff was simulated in replicate mesocosms by adding soil from an adjacent oak forest that had matured in water from the main river tributary of the lagoon. Automated high-frequency monitoring of dissolved oxygen, chlorophyll-a fluorescence, salinity, light, and temperature was combined with manual sampling of organic and inorganic nutrient pools, pH, carbonate chemistry and maximum quantum yield (Fv:Fm) of photosystem II (PSII). High-frequency data were used to estimate gross oxygen primary production (GPP), respiration (R), and phytoplankton growth (μ) and loss (L) rates. During the first half of the experiment (d2-d11), the simulated runoff reduced light availability (-52%), chlorophyll-a concentrations (-70%) and phytoplankton growth rates (-53%). However, phytoplankton maintained a certain level of primary production by increasing its photosynthetic efficiency. Meanwhile, the runoff enhanced R (+53%), shifting the metabolic status (GPP:R) of the system toward heterotrophy and increasing the partial pressure of carbon dioxide (pCO_2), potentially switching the direction of the air-sea CO_2 exchange. However, during the second part of the experiment (d11-d17), remineralised nutrients boosted phytoplankton growth (+299%) in the terrestrial runoff treatment, but not its loss rates, leading to phytoplankton biomass accumulation and suggesting a mismatch between phytoplankton and its predators. Our study showed that a simulated terrestrial runoff significantly affected key plankton processes, suggesting that climate change-related increases in runoff frequency and intensity can shift the metabolic balance of Mediterranean coastal lagoons toward heterotrophy.

https://doi.org/10.5194/egusphere-2023-2782
Preprint. Discussion started: 24 November 2023

1 Introduction

Climate change is predicted to increase the frequency and intensity of short extreme rainfall events in the Mediterranean region (Alpert *et al.* 2002, Sanchez *et al.* 2004). Consequently, the runoff of terrestrial matter will become more frequent in coastal Mediterranean waters. These runoffs constitute a pulse input of organic and inorganic nutrients into the water column and decrease light penetration (Nunes *et al.* 2009), substantially impacting marine ecosystems, and notably plankton communities (Deininger and Frigstad 2019, Striebel *et al.* 2023).

Plankton is crucial for aquatic ecosystems because it forms the basis of the aquatic food web and plays an important role in multiple biogeochemical cycles, notably that of oxygen (Falkowski *et al.* 2003, Falkowski 2012). Indeed, phytoplankton produces oxygen through its gross primary production (GPP), and all planktonic organisms consume it through aerobic respiration (R). Hence, assessing GPP and R provides a community metabolism index (GPP : R) and determines the capacity of an aquatic ecosystem to serve as a net producer or consumer of oxygen, and ultimately as a sink or releaser of atmospheric carbon dioxide (Lopez-Urrutia *et al.* 2006). This community metabolism index considerably depends on the fate of phytoplankton, which is itself related to phytoplankton growth (μ) and loss (L) rates. Therefore, assessing μ and L provides a trophic index (μ : L) related to the performance of both phytoplankton and its predators (Soulié *et al.* 2022a).

The consequences of terrestrial runoffs on plankton communities and associated processes remain unclear. The inputs of terrestrial carbon and nutrients have been shown to promote phytoplankton and bacteria in Mediterranean coastal waters (Pecqueur *et al.* 2011, Liess *et al.* 2016), possibly leading to higher GPP and R. However, this positive effect of nutrient enrichment can be mitigated by light attenuation resulting from the runoff, which can depress phytoplankton photosynthesis, and therefore GPP, as observed in the North Sea, Baltic Sea, and in a North Atlantic bay (Mustaffa *et al.* 2020, Paczkowska *et al.* 2020, Soulié *et al.* 2022b). The contradictory effects of light attenuation and nutrient enrichment induced by terrestrial runoffs on plankton metabolism can change the structure of planktonic communities and, ultimately, their related processes. They can favour bacteria over phytoplankton (Meunier *et al.* 2017, Andersson *et al.* 2018, Courboulès *et al.* 2023), large phytoplankton at the expense of smaller cells (Deininger *et al.* 2016, Mustaffa *et al.* 2020), and affect protozooplankton (Courboulès *et al.* 2023). Consequently, these shifts can alter plankton processes because the structure and functions of aquatic communities are closely related (Giller *et al.* 2004).

Although the consequences of terrestrial runoffs have been well-studied in freshwater systems, an important knowledge gap exists regarding the impacts of terrestrial runoffs on coastal marine ecosystems (Blanchet *et al.* 2022). In this regard, evaluating the consequences of terrestrial runoffs on plankton communities and processes in ecologically and economically important areas, such as coastal lagoons (Soria *et al.* 2022), enclosed systems that are often subject to inputs from the land, is of fundamental concern. In the present study, we conducted an *in situ* mesocosm experiment in the Mediterranean coastal Thau Lagoon, a shallow productive lagoon which hosts oyster farms and serves as a nursery for several wild fish species (La Jeunesse *et al.* 2015). Moreover, it is naturally subjected to storm-induced terrestrial runoffs (Pecqueur *et al.* 2011, Fouilland *et al.* 2012), notably in fall during the 'Cévenols' events, a meteorological phenomenon characterized by storms and heavy rainfalls

https://doi.org/10.5194/egusphere-2023-2782
Preprint. Discussion started: 24 November 2023

that usually cause flash-flooding in the Mediterranean coast (Ducrocq *et al*. 2008). Several mesocosms were used with half serving as control mesocosms and in the other half a terrestrial runoff was simulated by adding soil from an adjacent typical Mediterranean oak forest that maturated over two weeks in water from the Vène River, the main river tributary of the Thau Lagoon (Plus *et al*. 2006). The responses of all plankton food web compartments in the present experiment have been detailed by Courboulès *et al*. (2023). In the present study, high-frequency data from automated sensors immersed in the mesocosms were used to estimate GPP, R, µ and L in every mesocosm, and assess how both the metabolic and trophic indices of the community responded to the simulated runoff. Manual sampling was performed to assess dissolved and particulate materials as well as photosynthetic efficiency and carbonate system parameters.

2 Material and Methods

2.1 In situ mesocosm experimental set-up

An *in situ* mesocosm experiment was performed for 18 days in May 2021 in the Thau Lagoon using the facilities of the MEDIterranean platform for Marine Ecosystems Experimental Research (MEDIMEER, 43°24’53’’N, 3°41’16’’E). Thau Lagoon is a shallow coastal lagoon of 75 km^2 with a mean depth of 4 m and is located on the French coast of the Northwestern Mediterranean Sea (Derolez *et al.* 2020). Six mesocosms were established in the lagoon. Each mesocosm consisted of a bag made of nylon-reinforced 200 µm thick vinyl acetate polyethylene film which was 280 cm high and 120 cm wide (Insinööritoimisto Haikonen Ky, Sipoo, Finland). Each mesocosm was covered with a dome of polyvinyl-chloride to avoid external inputs and was equipped with a sediment trap. On May 3 (d0), all the mesocosms were filled simultaneously using a pump (SXM2/A SG, Flygt) with 2200 L of subsurface lagoon water preliminarily screened through a 1000 µm mesh to remove large particles and organisms. The water was pooled in a large container before being distributed simultaneously by gravity to the six mesocosms through parallel pipes. In each mesocosm, the water column was continuously homogenized with a pump (Rule, Model 360) immersed at a depth of 1 m, resulting in a turn-over rate of approximately 3.5 d^{-1}. Three mesocosms served as controls, while in three other maturated soil was added to simulate a terrestrial runoff event (these mesocosms are hereafter referred to as the “terrestrial runoff” treatment). For each treatment, one mesocosm displayed considerable differences in biological, physical, and chemical parameters compared to the two other replicates of the same treatment, most probably because of the malfunctioning of the mixing pumps, and it was therefore removed from the analysis. Data are therefore presented as the mean of the two replicates for each treatment ± the range of observations.

2.2 Soil extraction, preparation, and maturation

Two weeks before the beginning of the mesocosm experiment, soil was extracted from the Puéchabon state forest, a fully preserved typical Mediterranean oak forest located approximately 30 km north of the Thau Lagoon (43°44’29’’N, 3°35’45’’E)

https://doi.org/10.5194/egusphere-2023-2782
Preprint. Discussion started: 24 November 2023

(Allard *et al.* 2008). The soil was then roughly screened over a 1 cm mesh. On the same day as soil extraction, water was collected from the Vène River, the main tributary of the Thau Lagoon, which is known for its episodic flash floods (Pecqueur *et al.* 2011). Water was screened over a 200 µm mesh to remove large particles and organisms. The soil and river water were then mixed to reach a concentration of 416 g soil L^{-1}, which represents natural flash flood events occurring in the lagoon (Fouilland *et al.* 2012). This mixture was then left to mature for two weeks in transparent Nalgene carboys placed in an outdoor pool continuously supplied with natural water from the Thau Lagoon. During the maturation step, each carboy was homogenised and aerated daily. This maturation was performed to mimic the degradation process of the most labile compounds that naturally occurs during their transportation from the soil to coastal waters during natural runoff events (Müller *et al.* 2018). After the manual mesocosms sampling on May 4 (d1), 7 L of the soil solution was added to each of the three "runoff" mesocosms, representing a final concentration of 1.3 g soil L^{-1}. Further details regarding the choice and description of the soil addition protocol can be found in Courboulès *et al.* (2023).

2.3 Acquisition, calibration, and correction of the high-frequency sensor data

In each mesocosm, a set of high-frequency sensors was immersed to a depth of 1 m. Each set constituted of a fluorometer (ECO-FLNTU, Sea-Bird Scientific, United States) for Chl-*a* fluorescence, from which Chl-*a* concentration was derived, an oxygen optode (3835, Aanderaa, Bergen, Norway) for dissolved oxygen (DO) concentration and saturation, an electromagnetic induction conductivity sensor (4319, Aanderaa, Bergen, Norway) for salinity, a spherical underwater quantum sensor (Li-193, Li-Cor, United States) for the incident photosynthetically available radiation (PAR), and three water temperature probes (Thermistore Probe 107, Campbell Scientific, United States) installed at three different depths (0.5, 1 and 1.5 m). Each sensor recorded measurements every minute during the entire experiment. In the results section, the high-frequency data are presented as daily averages. The fluorometers, oxygen optodes, conductivity sensors, and temperature probes were calibrated before and after the experiment. In addition, Chl-*a* fluorescence and oxygen sensor data were corrected using discrete high-performance liquid chromatography (HPLC) and Winkler Chl-*a* and DO measurements, respectively. To do so, three borosilicate bottles (120 mL) were filled with water sampled from each mesocosm using a 5 L Niskin water sampler at depth of 1 m every other day in the morning. DO was immediately fixed by adding Winkler reagents (Carrit and Carpenter 1966). After at least 6 hr of fixation, the DO concentration in each bottle was measured with an automated Winkler titrator (Methrom 916-Ti-Touch) using a potentiometric titration method. Similarly, a polycarbonate bottle (2 L) was filled with water that was sampled every morning from each mesocosm using a Niskin water sampler at a depth of 1 m. Samples were then immediately filtered at low light conditions using a vacuum pump on glass-fibre filters (Whatman GF/F, 0.7 µm pore size). Filters were then stored at -80 °C until analyses with HPLC (Shimadzu) following the method by Zapata *et al.* (2000). Details of the calibration procedure can be found in the **Supplementary Information** and in Soulié *et al.* (2023).

https://doi.org/10.5194/egusphere-2023-2782
Preprint. Discussion started: 24 November 2023

2.4 Manual mesocosm sampling and monitoring for chemical variables

Each mesocosm was sampled daily using a 5 L Niskin water sampler at a depth of 1 m to monitor dissolved inorganic nutrients (nitrate + nitrite [NO_2^-+NO_3^-], ammonium [NH_4^+], orthophosphate [PO_4^{3-}], and silicate [SiO_2]), dissolved organic carbon (DOC), particulate organic carbon (POC), and nitrogen (PON) concentrations; and every second day to measure pH and total alkalinity (TA). For dissolved inorganic nutrient analyses, 50 mL sub-samples of mesocosm water were placed in acid-washed polycarbonate bottles. Directly after, these samples were filtered over 0.45 µm filters (Gelman Sciences, United States) and stored in high-density polyethylene tubes at -20°C until further analyses that were performed within 48 hr. Nitrate, nitrite, orthophosphate, and silicate analyses were performed with an automated colorimeter (Skalar Analytical, The Netherlands, Aminot and Kérouel 2007), and ammonium analyses were performed using the fluorometric method (Turner Design, module 7200-067-W, United States, Aminot *et al.* 1997, Holmes *et al.* 1999). For DOC analyses, 30 mL subsamples of mesocosm water were filtered through two pre-combusted (4h, 450°C) glass-fibre filters (Whatman GF/F), 90 µL of phosphoric acid (85% concentration) was then added and sub-samples were then stored at 4°C in the dark until further analyses, which were performed by high-temperature catalytic oxidation (HTCO) on a total organic carbon analyser (TOC-L-CSH, Shimadzu). For POC and PON analyses, sub-samples (0.5-1 L) of mesocosm water were filtered over pre-combusted (4h, 450°C) glass-fibre filters (Whatman GF/F). Filters were then placed in a stove at 60°C for at least 12h. The POC and PON concentrations were then measured using a CHN analyser (Unicube, Elementar). The samples for pH and TA determinations were collected in 300 mL borosilicate glasses bottles according to standard sampling methods for carbonate chemistry (Dickson *et al.* 2007). Samples for TA determination were filtered immediately on glass-fibre filters (Whatman GF/F, 0.45 µm pore size), spiked with 50 µL of $HgCl_2$ saturated solution and stored for later analysis. Samples for pH analysis were spiked with $HgCl_2$ and were analysed within 36 hr.

pH was measured spectrophotometrically (LAMBDA 365 UV/Vis, Perkins Elmer), on a "total scale" at 25.0°C (pH_{25}) with m-Cp as an indicator (reproducibility ± 0.002), according to Clayton and Byrne (1993) and Dickson *et al.* (2007) with replicate analysis for control and triplicate for treated mesocosms. TA was measured in the laboratories of CNR-ISMAR in Trieste (replicate analysis), using an open-cell potentiometric titration with a derivative determination of the end point, according to Hernandez-Ayon *et al.* (1999) (reproducibility ± 0.1 µmol kg^{-1}). Certified reference seawater for carbonate chemistry (provided by Prof A. G. Dickson, Scripps, California) was used for pH and TA analysis. The dissolved inorganic carbon (DIC) concentration, CO_2 partial pressure (pCO_2), and pH at *in situ* temperature (pH) were calculated using the CO2SYS program (Microsoft Excel version 2.5; Lewis and Wallace 1998, Pierrot *et al.* 2006), using the carbonate constants from Lueker *et al.* (2000) sulphate constants from Dickson (1990) and parameterization of borate from Lee *et al.* (2010).

https://doi.org/10.5194/egusphere-2023-2782
Preprint. Discussion started: 24 November 2023

2.5 Estimation of the Daily Light Integral from the high-frequency PAR sensor data

PAR measurements were used to calculate the Daily Light Integral (DLI). This value corresponds to the average quantity of light available for photosynthesis received by a 1 m^2 surface over a 24-h period (Soulié *et al.* 2022b). DLI was calculated using **Eq. 1** as follows:

$$DLI = \frac{mean\ PAR \times day\ length \times 3600}{1 \times 10^6}, \textbf{(Equation 1)}$$

where DLI is expressed in mol m^{-2} d^{-1}, mean PAR between sunrise and sunset in µmol m^{-2} s^{-1}, and day length in hr.

2.6 Estimation of µ and L from the high-frequency Chl-*a* sensor data

The high-frequency Chl-*a* data were used to estimate phytoplankton growth (µ) and loss (L) rates following a method detailed by Soulié *et al.* (2022a). First, the high-frequency Chl-*a* data were corrected for non-photochemical quenching as detailed in **Supplementary Information**. Then, each Chl-*a* cycle was separated into an "increasing period" and a "decreasing period". The "increasing period" started at sunrise until the maximum Chl-*a* fluorescence was reached, generally a few minutes to a few hours after sunset. The "decreasing period" started from this maximum until the next sunrise. For each period, an exponential fit was applied to the Chl-*a* data, and L was estimated form the decreasing period. Then, µ was estimated from the increasing period. The detailed calculations are presented in the **Supplementary Information**.

2.7 Estimation of GPP and R from the high-frequency DO sensor data

DO data were used to estimate daily GPP, R during the day (Rdaytime) and the night (Rnight), and daily R following the method detailed by Soulié *et al.* (2021). This method is derived from the free-water diel oxygen technique (Staehr *et al.* 2010), and was specially developed for mesocosm experiments and to consider variability in both the coupling between day-night and DO cycles and in the respiration occurring during the day and at night. Briefly, each DO cycle was separated into a "positive instantaneous net community production period" (during which DO increases) and a "negative instantaneous net community production period" (during which DO decreases). For each period, the DO was smoothed using a 5-point sigmoidal model. These smoothed data were then used to estimate oxygen metabolic parameters in two major steps. First, the oxygen exchange term between water and the atmosphere was calculated, considering its dependence on temperature and salinity. Then, instantaneous and daily metabolic parameters were estimated. A precise description of the method is provided by Soulié *et al.* (2021) and the **Supplementary Information**.

https://doi.org/10.5194/egusphere-2023-2782
Preprint. Discussion started: 24 November 2023

2.8 Maximum photosystem II quantum yield measurements

Phytoplankton photosynthetic performance was estimated based on the fluorescence of the photosystem II (PSII). Subsamples of 1.5 mL from the Niskin water sampler were collected daily and analysed using a portable Pulse Amplitude Modulation fluorometer (Aquapen C AP 110 C, Photon System Instruments, Czech Republic). The maximum quantum yield of photosynthesis ($F_v : F_m$) was measured after a 30-min acclimation period in the dark to ensure that all photosystem-II reactional centres were open. The measurement was done using the 'OJIP' protocol and an excitation wavelength of 450 nm (Strasser *et al.* 2000).

2.9 Heterotrophic bacterial abundance measurements

Heterotrophic bacterial abundance was assessed daily using flow cytometry. For this purpose, 1.5 mL samples were collected from the Niskin water sampler and fixed using glutaraldehyde (Grade I, Sigma; 4% final dilution), and then frozen into liquid nitrogen before being maintained at -80°C until further analyses. The samples were stained with SYBR Green I (S7563, Invitrogen; 0.25% final dilution) (Marie *et al.* 1997). Analyses were performed using a FACSCanto2 flow cytometer (Becton-Dickinson; set at low speed for 3 min), and internal cell size standards (cytometry fluorescent beads, Polysciences Inc.) of 1 and 2 µm diameter were added to each run. Bacterial populations were identified and counted via stained green fluorescence (530/30 nm) and relative side scatter (Courboulès *et al.* 2021, 2023).

2.10 Statistical analyses

To test the difference between the control and terrestrial runoff treatments, we performed Repeated-Measures Analyses of Variances (RM-ANOVA) with the treatment as a fixed factor and time as a random factor (*nlme* package, R software) over the entire experiment (after the addition of soil, d2-d18) and over shorter periods to assess specific trends. Data from d1 were not included in the statistical analyses as sampling was performed before adding the soil, simulating the terrestrial runoff, in the runoff mesocosms. Statistical significance was set at $p < 0.05$. Before performing the RM-ANOVAs, the assumptions of homoscedasticity and normality were checked using the Levene and Shapiro-Wilk tests, respectively. When these assumptions were not met even after transforming the data (log- or square-root transformation), a non-parametric Kruskal-Wallis test was performed instead of RM-ANOVA. The non-parametric Spearman's correlation coefficient was used to assess significant ($p < 0.05$) relationships between the Logarithm Response Ratio (LRR) of the variables. All data management and statistical analyses were performed using the R software (version 4.0.1).

https://doi.org/10.5194/egusphere-2023-2782
Preprint. Discussion started: 24 November 2023

3 Results

3.1 Effects of the terrestrial runoff treatment on physical and chemical conditions

In the control treatment, the water temperature varied from 16.68 ± 0.16 °C to 17.95 ± 0.65 °C (**Fig. 1a**), and was not significantly different in the terrestrial runoff treatment compared to the control (**Table 1**). The salinity was on average 38.42 ± 0.11 in the control treatment, increasing almost continuously throughout the experiment (**Fig. 1b**). In the terrestrial runoff treatment, the salinity was significantly reduced by 0.7% (**Table 1**). Similarly, the DLI was, on average, 18.65 ± 1.45 mol m^{-2} d^{-1} in the control treatment (**Fig. 1c**). The terrestrial runoff drastically decreased it, by 76% on d2 and by, on average, 43% over the entire experiment. This negative effect was stronger during the first half of the experiment (52% from d2 to d11), and was attenuated during the second half of the experiment (27% from d12 to d18) (**Table 1**). In the control treatment, pH varied from 8.10 ± 0.05 to 8.19 ± 0.01 (**Fig. 1d**), decreasing from d1 to d10 before stabilisation until the end of the experiment. In the runoff treatment, it was significantly reduced by 0.4% (8.06 ± 0.01 to 8.19 ± 0.01) (**Table 1**). In addition, pCO_2 ranged from 292.49 ± 0.45 to 368.27 ± 43.97 µatm in the control treatment (**Fig. 1e**). In the runoff treatment, it was significantly higher by 9% compared to the control, despite returning to the control level by the end of the experiment (**Table 1**). The DOC concentrations were on average 1.70 ± 0.10 mg L^{-1} in the control treatment (**Fig. 1f**). In the terrestrial runoff treatment, DOC concentrations were not immediately enhanced after the addition of soil, reaching higher concentrations only in the middle and end of the experiment. However, no significant differences were observed between the treatments (**Table 1**). The DIC concentrations ranged from 2184.04 ± 14.89 to 2230.44 ± 0.76 µmol Kg^{-1} (**Fig. 1g**). They were significantly higher by 1% in the runoff treatment than in the control, with the highest difference between treatments on d2 (3%) (**Table 1**). The POC + PON concentrations displayed similar dynamics over time. The POC concentrations ranged from 0.26 ± 0.01 mg L^{-1} to 0.55 ± 0.09 mg L^{-1} (**Fig. 1h**), whereas the PON concentrations ranged from 0.04 ± 0.01 mg L^{-1} to 0.07 ± 0.01 mg L^{-1} (**Fig. 1i**). They were both significantly enhanced by 32-50% by the terrestrial runoff at the beginning of the experiment (d2 to d12), then decreased to the level of the control (**Table 1**). The concentrations of dissolved inorganic nutrients exhibited different trends. The nitrate + nitrite concentrations ranged from 0.29 ± 0.03 µM to 0.50 ± 0.01 µM in the control treatment, and were not significantly affected by the terrestrial runoff (**Fig. 1j**, **Table 1**). Conversely, while the ammonium concentrations remained relatively constant in the control treatment, ranging from 0.02 ± 0.01 µM to 0.12 ± 0.07 µM, they increased significantly in the terrestrial runoff treatment, reaching 0.96 ± 0.04 µM on d10, before decreasing to the control level on d16 (**Fig. 1k**, **Table 1**). The orthophosphate concentrations ranged from 0.03 ± 0.01 µM to 0.07 ± 0.01 µM in the control treatment, with peaks at the beginning and the end of the experiment (**Fig. 1l**). They were significantly higher in the terrestrial runoff treatment, but only in the middle of the experiment (63% from d10 to d13) (**Table 1**). Finally, the silicate concentrations ranged from 0.52 ± 0.15 µM to 0.79 ± 0.19 µM in the control treatment, they decreased on d2 before remaining relatively constant throughout the experiment (**Fig. 1m**). They were significantly higher in the terrestrial runoff treatment during the entire experiment by 214% (**Table 1**).

https://doi.org/10.5194/egusphere-2023-2782
Preprint. Discussion started: 24 November 2023

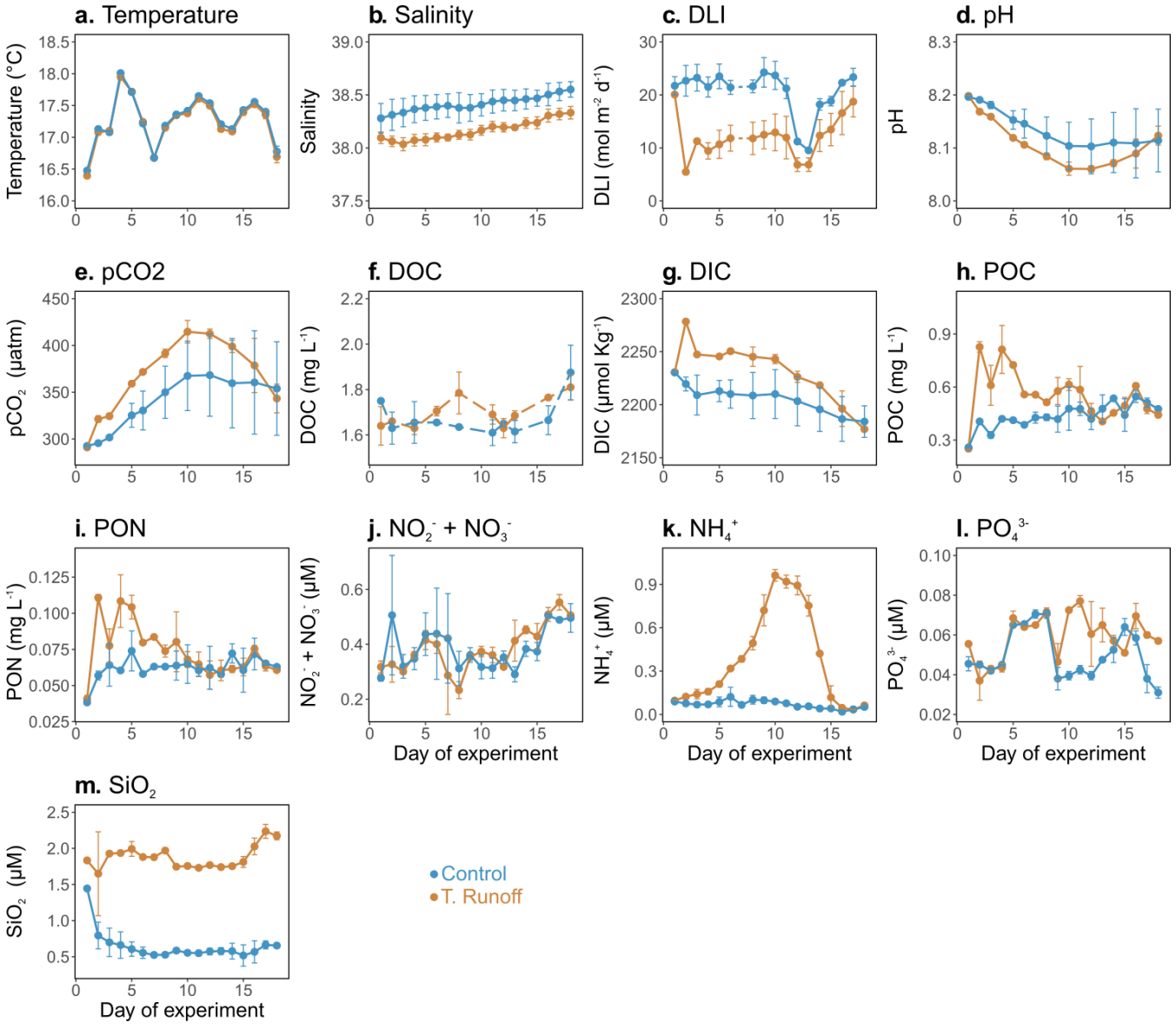

Figure 1. Daily average temperature (a), salinity (b), daily light integral (DLI, c), pH (d), pCO_2 (e), dissolved organic carbon concentrations (DOC, f), dissolved inorganic carbon concentrations (DIC, g), particulate organic carbon concentrations (POC, h), particulate organic nitrogen concentrations (PON, i), nitrate + nitrite concentrations (NO_2^-+NO_3^-, j), ammonium concentrations (NH_4^+, k), orthophosphate concentrations (PO_4^{3-}, l), and silicate concentrations (SiO_2, m) in the control (blue) and terrestrial runoff (gold) treatments. Error bars represent the range of the observations.

3.2 Effects of the terrestrial runoff treatment on bacterial abundances

In the control treatment, bacterial abundances ranged from $0.8 \times 10^6 \pm 0.3 \times 10^6$ to $1.9 \times 10^6 \pm 0.8 \times 10^6$ cells mL^{-1} (**Fig. 2**). They were significantly higher in the runoff treatment from d2 to d8 (59%) and from d15 to d18 (51%), whereas they were

https://doi.org/10.5194/egusphere-2023-2782
Preprint. Discussion started: 24 November 2023

significantly lower in the middle of the experiment (-47% from d9 to d14) (**Table 1**). As a consequence, no significant differences were observed throughout the entire experiment.

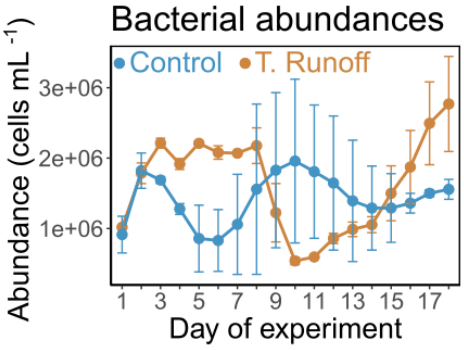

Figure 2. Daily average bacterial abundances in the control (blue) and terrestrial runoff (gold) treatments. Error bars represent the range of the observations.

3.3 Effects of the terrestrial runoff treatment on phytoplankton: Chl-a, growth and loss rates

In the control treatment, the Chl-*a* concentrations ranged from 0.83 ± 0.30 µg L^{-1} to 1.91 ± 0.45 µg L^{-1} (**Fig. 3a**). They remained relatively constant during the first half of the experiment, before increasing from d11 to d13, and then decreasing until the end of the experiment. In the terrestrial runoff treatment, they were significantly lower, particularly during the first part of the experiment (70% from d2 to d11) (**Table 1**). However, at the end of the experiment, they increased rapidly from d11 to d15, even surpassing the control level.

In the control, µ ranged from 0.06 ± 0.04 d^{-1} to 0.64 ± 0.06 d^{-1}, peaking on d4, d7 and d12 (**Fig. 3b**). In the terrestrial runoff treatment, it was significantly lower than in the control by an average of 53% from d2 to d10 (**Table 1**). However, it increased drastically during the second half of the experiment, and was significantly almost three times higher than in the control from d12 to d17. L varied from 0.19 ± 0.12 d^{-1} to 0.95 ± 0.05 d^{-1} in the control treatment, and was relatively constant and generally higher than 0.2 d^{-1} (**Fig. 3c**). In the terrestrial runoff treatment, it was significantly lower than in the control by an average of 32% throughout the experiment, and by 60% from d3 to d14 (**Table 1**). However, it was higher than in the control from d1 to d3, and came back to the control level at the end of the experiment. As a consequence of the generally higher L than µ in the control, the µ:L ratio was below 1 on 13 out of the 16 days (**Fig. 3d**). It ranged from 0.10 ± 0.06 to 2.76 ± 2.26. The terrestrial runoff significantly increased the µ:L ratio by an average of 305% over the entire experiment (**Table 1**). The greatest difference between treatments was found on d13, when the ratio was almost 11 times higher in the terrestrial runoff than in the control treatment.

https://doi.org/10.5194/egusphere-2023-2782
Preprint. Discussion started: 24 November 2023

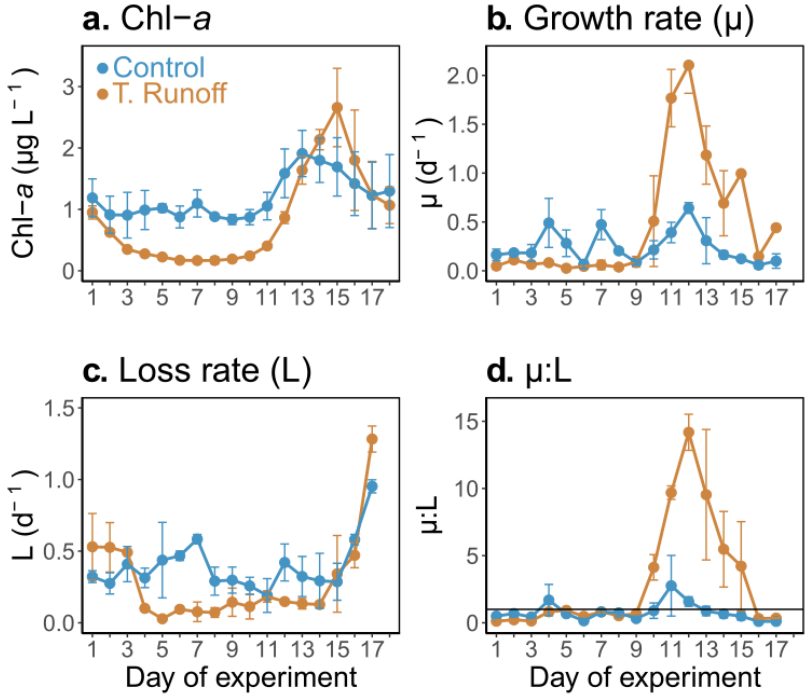

Figure 3. Daily average chlorophyll-*a* (Chl-*a*, a), phytoplankton growth rate (µ, b), phytoplankton loss rate (L, c), and growth : loss ratio (µ:L, d) in the control (blue) and terrestrial runoff (gold) treatments. Error bars represent the range of the observations. Note that µ and L could not be estimated on d18 owing to the lack of a complete fluorescence cycle.

3.4 Effects of the terrestrial runoff treatment on primary production, respiration, and photosynthetic efficiency

In the control treatment, GPP ranged from 0.26 ± 0.02 to 0.78 ± 0.03 gO_2 m^{-3} d^{-1} (**Fig. 4a**). After decreasing from d1 to d2, it increased until it reached its maximum on d7, and then decreased relatively continuously until the end of the experiment. In the terrestrial runoff treatment, it increased significantly by an average of 37% at the middle of the experiment, from d9 to d14 (**Table 1**). When the GPP was normalised by the daily Chl-*a* concentration, it was significantly higher in the terrestrial runoff treatment than in the control by an average of 312% throughout the experiment (**Fig. 4b**).

In the control treatment, R ranged from 0.18 ± 0.01 to 0.67 ± 0.02 gO_2 m^{-3} d^{-1}, and it showed a similar dynamic as GPP (**Fig. 4c**). It was significantly enhanced in the terrestrial runoff treatment by an average of 46% over the entire experiment (**Table 1**).

The GPP : R ratio ranged from 0.94 ± 0.12 to 1.69 ± 0.19 in the control treatment, and it was higher than 1 on 16 out of 17 days (**Fig. 4d**). In the terrestrial runoff treatment, it decreased significantly by an average of 32% during the first half of the experiment (d2-d10), before increasing and reaching the control level during the second half of the experiment (**Table 1**). Consequently, it was higher than 1 only on 10 out of the 17 days.

https://doi.org/10.5194/egusphere-2023-2782
Preprint. Discussion started: 24 November 2023

In the control, the maximum PSII quantum yield, an indicator of the maximum potential photosynthetic capacity, ranged from 0.24 ± 0.01 to 0.55 ± 0.04 (**Fig. 4e**). It was not significantly different between the treatments over the entire experiment; however, it increased significantly by 43% in the terrestrial runoff treatment from d8 to d11 (**Table 1**).

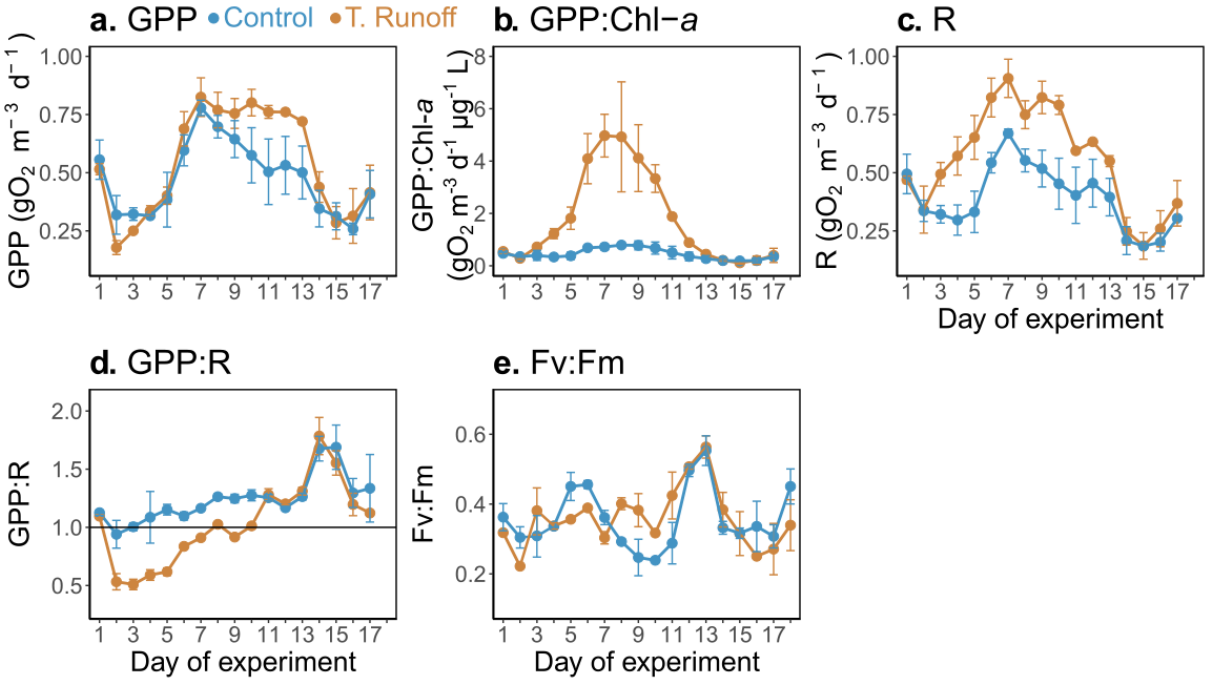

Figure 4. Daily average gross primary production (GPP, a), GPP normalised by chlorophyll-*a* (GPP:Chl-*a*, b), community respiration (R, c), GPP : R ratio (d), and maximum quantum yield (F_v : F_m) of photosystem II (PSII) (e) in the control (blue) and terrestrial runoff (gold) treatments. Error bars represent the range of the observations. Note that GPP and R could not be estimated on d18 owing to the lack of a complete oxygen cycle.

Table 1. Summary table of the statistical comparison and the % relative change between the terrestrial runoff and the control treatments. The significance level was set to 0.05 and significant P-values, as well as their corresponding relative change, were highlighted in bold. When a RM-ANOVA was performed, its F value was given in brackets, and when a Kruskal-Wallis was performed instead, "KW" was indicated.

Parameter	Period	P-value	% difference
Temperature	2-18	0.64 (KW)	-0.2
Salinity	2-18	**< 1×10^{-4}** ($F_{1,16}$=1035)	**-0.7**
DLI	2-18	**1.4×10^{-3}** (KW)	**-43.3**
	2-11	**9.1×10^{-4}** (KW)	**-51.6**
	12-18	**1.4×10^{-3}** ($F_{1,6}$=32.9)	**-27.3**
pH	2-18	**3×10^{-4}** ($F_{1,9}$=32.4)	**-0.4**
pCO_2	2-18	**4×10^{-4}** ($F_{1,9}$=30.5)	**8.9**
DOC	2-18	0.27 (KW)	0.4
DIC	2-18	**7×10^{-4}** ($F_{1,9}$=25.3)	**1.3**

https://doi.org/10.5194/egusphere-2023-2782
Preprint. Discussion started: 24 November 2023

POC	2-18	**2.2×10^{-6}** ($F_{1,16}$=11.5)	**27.8**
	2-12	**1.1×10^{-8}** ($F_{1,10}$=27.9)	**49.3**
	12-18	0.621 (KW)	-2.0
PON	2-18	**0.001** (KW)	**18.8**
	2-12	**1.6×10^{-5}** ($F_{1,10}$=12.9)	**32.3**
	12-18	0.474 ($F_{1,6}$=0.7)	-2.7
$NO_2^- + NO_3^-$	2-18	0.75 ($F_{1,16}$=0.1)	1.3
NH_4^+	2-18	**3.2×10^{-4}** (KW)	**486.5**
PO_4^{3-}	2-18	**0.02** ($F_{1,16}$=6.8)	**18.0**
	10-13	**8.4×10^{-3}** ($F_{1,3}$=38.7)	**62.7**
SiO_2	2-18	**5.4×10^{-7}** (KW)	**213.7**
GPP	2-17	0.37 (KW)	16.1
	9-14	**1.1×10^{-3}** ($F_{1,5}$=44.7)	**36.6**
	12-17	0.08 ($F_{1,15}$=4.8)	24.5
GPP : Chl-*a*	2-17	**0.02** (KW)	**312.1**
R	2-17	**$<1\times10^{-4}$** ($F_{1,15}$=38.4)	**45.7**
	2-11	**2×10^{-4}** ($F_{1,10}$=32.7)	**52.5**
GPP : R	2-17	**7×10^{-4}** ($F_{1,15}$=18.4)	**-17.6**
	2-10	**$<1\times10^{-4}$** ($F_{1,15}$=82.5)	**-32**
F_v : F_m	2-17	0.94 ($F_{1,17}$=0.01)	0.4
	8-11	**3.7×10^{-3}** ($F_{1,5}$=68.7)	**43.0**
Bacterial abundances	2-18	0.183 (KW)	15.0
	2-8	**1.3×10^{-4}** ($F_{1,6}$=37.2)	**59.0**
	9-14	**2.5×10^{-3}** ($F_{1,5}$=24.2)	**-47.0**
	15-18	**6.7×10^{-3}** ($F_{1,3}$=22.7)	**51.0**
Chl-*a*	2-18	**1.2×10^{-3}** ($F_{1,17}$=14.9)	**-30.2**
	2-11	**1.6×10^{-4}** (KW)	**-70.2**
	12-18	0.89 ($F_{1,8}$=0.02)	4.2
Growth rate (μ)	2-17	0.86 ($F_{1,15}$=0.03)	110.6
	2-11	**0.02** ($F_{1,8}$=7.5)	**-52.8**
	12-17	**3.0×10^{-4}** ($F_{1,5}$=77.9)	**298.7**
Loss rate (L)	2-17	**4.7×10^{-3}** ($F_{1,15}$=11)	**-32.1**
	3-14	**6×10^{-4}** ($F_{1,11}$=22.3)	**-60.0**
μ : L ratio	2-17	**0.02** ($F_{1,15}$=7.3)	**305.4**
	11-18	**1×10^{-4}** ($F_{1,5}$=115)	**550.3**

3.5 Correlation matrix between the responses of phytoplankton processes, community metabolism, and environmental variables

To assess the relationships between the effects of the terrestrial runoff on various variables, Spearman's correlations were calculated between the LRR of phytoplankton processes, community metabolism and environmental variables. All significant correlations are shown in the matrix (**Fig. 5**). GPP was positively correlated with NH_4^+ and PO_4^{3-} concentrations, and negatively

https://doi.org/10.5194/egusphere-2023-2782
Preprint. Discussion started: 24 November 2023

correlated with bacteria abundance and POC+PON concentrations. R was positively correlated with pCO_2 and POC+PON concentrations, while being negatively correlated with μ, Chl-*a*, salinity, DLI and pH. In addition, μ was positively correlated to L, Chl-*a*, salinity, DLI, NO_2^-+NO_3^-, and negatively to bacterial abundances and POC+PON concentrations. Similarly, L was positively correlated with Chl-*a* and salinity, and negatively correlated with pCO_2. In addition, Chl-*a* was positively correlated with salinity, DLI and NO_2^-+NO_3^-, and negatively correlated with POC+PON, while bacterial abundances were positively correlated with DOC, and negatively correlated with NO_2^-+NO_3^-, NH_4^+ and PO_4^{3-}. Among environmental variables, it should be noted that DLI and POC+PON concentrations were negatively correlated, and NH_4^+ and PO_4^{3-} were positively correlated.

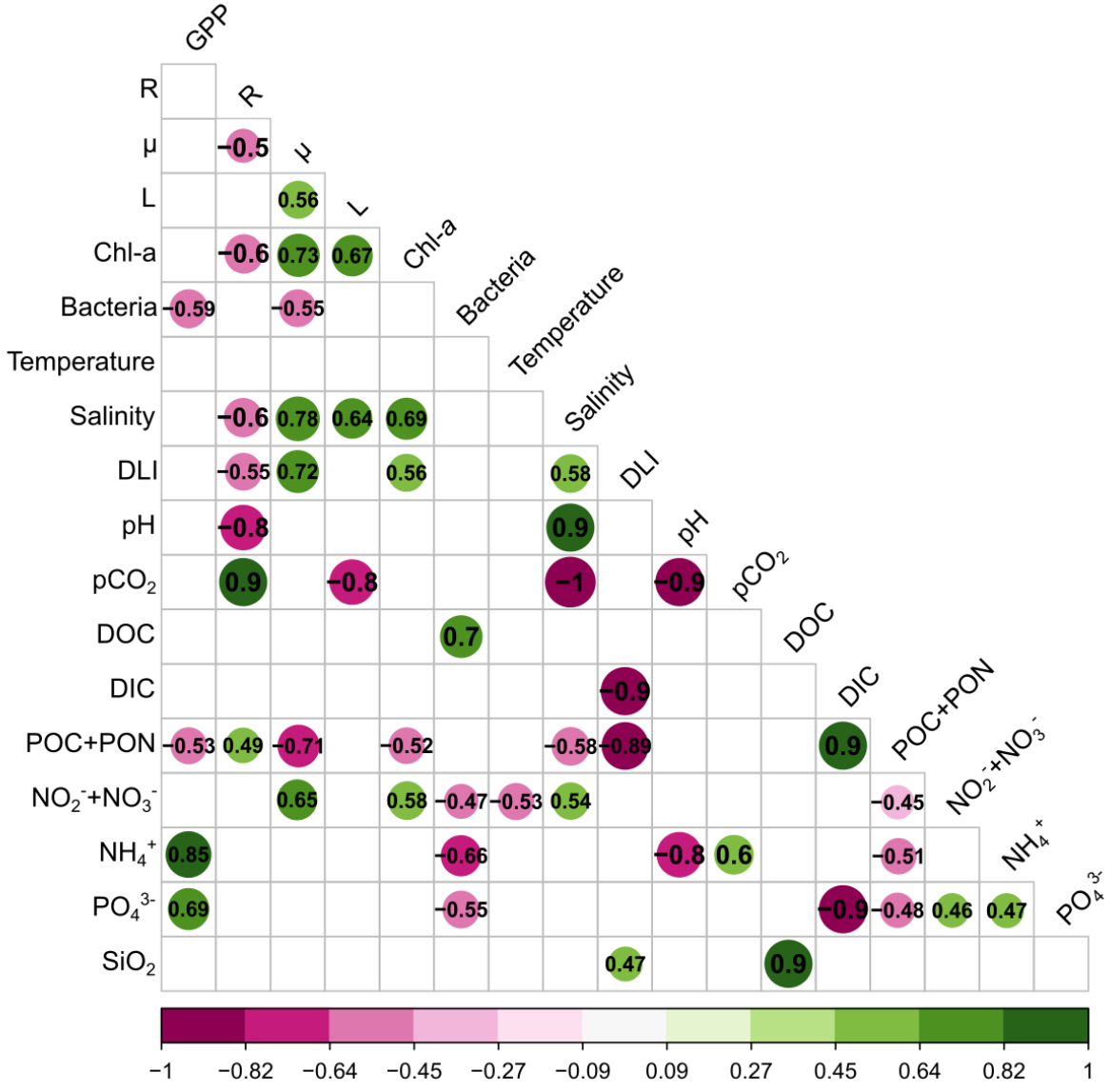

https://doi.org/10.5194/egusphere-2023-2782
Preprint. Discussion started: 24 November 2023

Figure 5. Correlation matrix based on Spearman's correlations between the log response ratio (LRR) of phytoplankton processes, community metabolism, and environmental variables. Only significant ($p < 0.05$) correlations are shown in the matrix. Green illustrates positive correlations and purple negative correlations. (GPP: Gross Primary Production, R: Respiration, Chl-*a*: Chlorophyll-*a*, µ: Growth rate, L: Loss rate, DLI: Daily Light Integral, DOC: Dissolved Organic Carbon, Dissolved Inorganic Carbon, POC + PON: Particulate Organic Carbon + Nitrogen).

4 Discussion

4.1 The terrestrial runoff depressed phytoplankton processes and shifted the metabolic balance of the system toward heterotrophy during the first half of the experiment

The present study aimed to evaluate the effects of a simulated terrestrial runoff on key plankton processes in a coastal Mediterranean lagoon. During the first half of the experiment (d2-d11), the simulated terrestrial runoff strongly decreased available light (-52%), consequently depressing phytoplankton biomass (-70%) and growth rate (-53%), as highlighted by the strong positive correlations between light availability, Chl-*a* and phytoplankton growth. This negative effect of light limitation induced by the runoff on phytoplankton biomass is consistent with a mesocosm experiment performed in the Baltic Sea where terrestrial organic matter addition reduced phytoplankton biomass through light attenuation (Mustaffa *et al.* 2020) and, generally, with a meta-analysis conducted on 108 studies reporting an average 23% reduction in photoautotroph biomass in response to experimentally reduced light across various freshwater and coastal ecosystems (Striebel *et al.* 2023). However, in the Thau Lagoon, a previous experiment reported a positive effect of soil addition, simulating a terrestrial runoff, on phytoplankton (Deininger *et al.* 2016). Nevertheless, the sinking of the added soil during the experiment performed by Deininger *et al.* (2016) might have rapidly lessen light attenuation, possibly releasing phytoplankton from the negative effect of light limitation. In addition, the experiment was conducted in late spring / early summer, when light is oversaturating (Trombetta *et al.* 2019), whereas our experiment was performed in spring, when light could be naturally more limiting for phytoplankton metabolism. Finally, Deininger *et al.* (2016) used a resin in their soil extraction procedure, yielding higher inorganic and organic nutrient concentrations in their extract compared to the protocol performed in the present study but being farther from natural terrestrial runoffs (Scharnweber *et al.* 2021). This emphasises the need for extreme caution when comparing experimental studies investigating terrestrial runoff effects because protocols are often different from one study to another.

In the present study, the lower phytoplankton biomass and growth rate in the runoff treatment were coupled with an overall decrease in phytoplankton loss rate from d3 until d14 (-60%). Phytoplankton loss could be caused by multiple factors that occur concomitantly, including: grazing by predators, viral lysis, sedimentation and natural death (Landry and Hassett 1982, Brussaard 2004). As the terrestrial runoff induced a negative effect on phytoplankton biomass during the first half of the experiment, it may have led to lower prey availability for its predators, resulting in a lower phytoplankton loss rate. This is supported by the negative effect of the simulated runoff on protozooplankton abundances reported in the present experiment

https://doi.org/10.5194/egusphere-2023-2782
Preprint. Discussion started: 24 November 2023

(Courboulès *et al.* 2023), which may be due to both lower phytoplankton abundance and higher grazing pressure from metazooplankton. Finally, the lower phytoplankton loss rate suggests that terrestrial runoffs could have important consequences for the entire plankton food web of coastal Mediterranean waters by disrupting phytoplankton loss processes, including grazing which the first link in the herbivorous food web (Legendre and Rassoulzadegan 1995, Mostajir *et al.* 2015). In contrast to phytoplankton biomass and growth, the gross primary production returned quickly to the control level (d4), and was even enhanced by the terrestrial runoff after a few days. This result was unexpected considering that oxygen production strongly depends on light, which was reduced by the runoff. However, we showed that the primary production to Chl-*a* ratio increased by more than three times in the runoff treatment, suggesting a strong enhancement of the phytoplankton photosynthetic efficiency to cope with lower light availability. Supporting this, the maximum PSII quantum yield, an indicator of the maximum potential photosynthetic activity (Strasser *et al.* 2000), increased significantly in the middle of the experiment in the terrestrial runoff treatment, further suggesting an increase in photosynthetic efficiency under light attenuation induced by the runoff. Moreover, this mismatch between oxygen production and carbon fixation, which has already been reported in a mesocosm experiment in Antarctic coastal waters (Deppeler *et al.* 2018), might be explained by the fact that photosynthetic carbon fixation is a two-stage process. The first is the conversion of light to energy in the chloroplast which produces oxygen as a by-product, and the second is the use of the produced energy to convert carbon dioxide into sugars through the Calvin cycle with the RuBisCO enzyme. Under stress conditions, the energy produced can also be used in alternative pathways other than carbon dioxide conversion, mainly respiration and photoacclimation (Behrenfeld *et al.* 2004, Halsey *et al.* 2010). Hence, we hypothesised that in the runoff treatment, a significant part of the energy produced by photosynthesis was not converted to growth, but was used instead in alternative pathways, explaining the observed mismatch between oxygen production and phytoplankton biomass. An alternative hypothesis is that the high quantity of particulate matter added through the simulated runoff induced a strong sedimentation of a part of the phytoplankton community toward the bottom of the mesocosm enclosures (Kiorboe *et al.* 1990). This sedimentation could have partly contributed to the mismatch between GPP and Chl-*a*, as sedimented phytoplankton could have continued to produce oxygen, while being undetected by both manual and sensor monitoring of Chl-*a*. Such sedimentation has already been suggested after heavy loadings of terrestrial matter during a natural flash flood event in Thau Lagoon, during which most of the microbial production may have been exported through sedimentation (Fouilland *et al.* 2012).

Simultaneously, community respiration was strongly enhanced (+53%) by the simulated terrestrial runoff. In marine waters, planktonic bacterial respiration is generally assumed to represent a major part of community respiration (Robinson 2008). In the present study, bacterial abundance was significantly enhanced by the runoff during the first part of the experiment (d2-d9), which is congruent with the higher respiration at that time. However, bacterial abundances then significantly decreased during the middle of the experiment (d9-d14) in the runoff treatment, while respiration remained significantly higher than in the control treatment, suggesting that respiration was mostly not sustained by bacteria at that time of the experiment, but by other biological compartments instead. Because Chl-*a* was still strongly depressed by the runoff during this period of the experiment, the hypothesis of an increase in phytoplankton respiration is not plausible. An increase in zooplankton respiration might instead

https://doi.org/10.5194/egusphere-2023-2782
Preprint. Discussion started: 24 November 2023

explain the positive effect on community respiration, as the abundance of some groups of metazooplankton was significantly enhanced by the runoff treatment (Courboulès *et al.* 2023), and the concomitant increase in PO_4^{3-} suggests a strong phosphorus excretion from zooplankton (Andersen *et al.* 1986, Vadstein *et al.* 1995).

As a consequence of the faster and greater increase in respiration compared to that in gross primary production, the terrestrial runoff resulted in a decrease in the production to respiration ratio and a shift toward heterotrophy of the metabolic index of the planktonic system during the first half of the experiment, as similarly reported after simulating a terrestrial runoff in a tropical reservoir (Trinh *et al.* 2016). Concomitantly, pCO_2 was significantly higher in the terrestrial runoff treatment, certainly because of the higher respiration as the responses of both variables were strongly correlated. These results are consistent with a study of 15 Swedish lakes that reported higher respiration leading to switches toward a heterotrophic metabolic index and increased pCO_2 in response to increased terrestrial carbon runoffs (Ask *et al.* 2012). Therefore, the present experiment shows, for the first time to our knowledge in Mediterranean coastal lagoons, that terrestrial runoffs could potentially shift coastal Mediterranean lagoons from being net oxygen producers to net oxygen sinks. Therefore, the respiration-driven gain in CO_2 can temporarily change the magnitude and direction of the air-sea CO_2 exchange, potentially switching the ecosystem from a CO_2 sink to a CO_2 source for the atmosphere.

4.2 Enhanced nutrient availabilities boosted phytoplankton processes during the second half of the experiment

During the second half of the experiment (d12-18), the phytoplankton biomass and processes increased in the terrestrial runoff treatment, in contrast to what occurred during the first half of the experiment. This might be explained by the higher dissolved inorganic nutrient availabilities in the runoff treatment, as the NH_4^+ and PO_4^{3-} concentrations were significantly higher in the terrestrial runoff treatment in the middle of the experiment, before being consumed and returning to the control level. The higher NH_4^+ concentrations possibly resulted from bacterial remineralization, as NH_4^+ is mostly produced by bacterial remineralisation of organic matter in coastal waters (Nixon 1981, Glibert 1982). In contrast, the higher PO_4^{3-} availability could be linked to grazing on bacteria, as grazers feeding upon bacteria generally show high phosphorus excretion rates (Andersen *et al.* 1986).

Enhanced nutrient availabilities may have fuelled phytoplankton growth to such an extent that the positive effect of nutrient availability surpassed the negative effect of light attenuation. This result suggests a trade-off mechanism between light and nutrient availabilities, whereby phytoplankton metabolism is enhanced or depressed depending on the extent of nutrient enrichment compared to the light attenuation associated with terrestrial runoffs. This mechanism has already been reported for northern lakes (Klug 2002, Isles *et al.* 2021) and even during mesocosm experiments evaluating the addition of dissolved organic matter into coastal waters of various regions (Deininger *et al.* 2016, Traving *et al.* 2017, Andersson *et al.* 2023). The present study provides additional support for this mechanism in Mediterranean coastal waters, and highlights the importance of considering it when modelling their response to terrestrial runoffs.

https://doi.org/10.5194/egusphere-2023-2782
Preprint. Discussion started: 24 November 2023

As mentioned earlier, Chl-*a* strongly increased during the second part of the experiment in the runoff treatment. This accumulation of phytoplankton biomass was related to the strong increase in phytoplankton growth rate from d10, while the phytoplankton loss rate remained low until the end of the experiment. Consequently, the growth to loss ratio was significantly enhanced by more than ten times compared to that of the control. This suggests an uncoupling between phytoplankton growth and its loss factors, such as zooplankton and/or viruses, at that time in the experiment, possibly because phytoplankton grew too quickly compared to its predators. Nonetheless, this emphasises the potentially substantial structural impacts of terrestrial runoff on plankton communities and their intricate interactions within aquatic food webs, as recently documented in lakes (Strandberg *et al.* 2023).

Even though the results of the present study come from a single mesocosm experiment, implying that their generalisation should be implemented with care, they emphasise the importance of considering the effects of terrestrial runoffs on plankton-mediated processes in modelling projections of Mediterranean coastal waters under future climate scenarios.

5 Data availability

The data used in this paper are openly available in the SEANOE repository at https://www.seanoe.org/data/00861/97260/ (Soulié *et al.* 2023).

6 Acknowledgements

We thank David Parin, Romain Michel, Hervé Violette, Kilian Terrier, Inès Garcia, Valentin Kempf, and Paul Verzele, from MEDIMEER, for their help with the mesocosms and sensors setup, daily sampling, and analyses of chemical variables. We acknowledge Eftihis Nikiforakis for his help with discrete oxygen measurements and daily sampling. We also thank David Pecqueur, the SU/CNRS BioPIC Imaging and Cytometry platform and Barbara Marie, from the Observatoire Océanologique de Banyuls/Mer, for the cytometric and the dissolved organic carbon analyses, respectively. We are grateful to Valerio Caruso from CNR-ISMAR for his valuable help in performing the total alkalinity analysis. We also thank the staff from the Puéchabon state forest for their help with practicalities during the sampling of soil. This work was part of the RESTORE project, funded by the French National Research Agency under the grant n°ANR-19-CE32-0013. C.C. was funded by the Transnational Access of the AQUACOSM-Plus project, which received funding from the European Union's Horizon 2020 research and innovation program under grant agreement n° 871081. As C.C. is a member of the JERICO-S3 project, which received funding from the European Union's Horizon 2020 research and innovation program under grant agreements n° 871153 and n° 951799, her contribution to this work is also part of her contribution to JERICO-S3. A CC-BY public copyright license has been applied by the authors to the present document and will be applied to all subsequent versions up to the Author Accepted Manuscript arising from this submission, in accordance with the grant's open access conditions.

https://doi.org/10.5194/egusphere-2023-2782
Preprint. Discussion started: 24 November 2023

7 Author contribution

F.Vi. and B.M. designed the mesocosm experiment, and F.Vi., S.M., and B.M. managed it. F.Vi., J.C., M.H., S.M., F. Vo., C.C., F.J. and B.M. participated in the daily sampling of the experiment. C.C. performed the analysis of pH, pCO_2, and dissolved inorganic carbon, with the help of F.Vo. T.S. processed the sensor data, made all related analyses, and wrote the original draft of the manuscript, with inputs from all authors. All authors read and approved the final version of the manuscript.

8 Competing interests

The authors declare that they have no conflict of interest.

9 References

Allard, V., Ourcival, J. M., Rambal, S., Joffre, R., and Rocheteau, A.: Seasonal and annual variation of carbon exchange in an evergreen Mediterranean forest in southern France. *Glob. Change Biol.* **14**: 714-725, https://doi.org/10.1111/j.1365-2486.2008.01539.x, 2008.

Aminot, A., Kirkwood, D. S., and Kérouel R.: Determination of ammonia in seawater by the indophenol-blue method: Evaluation of the ICES NUTS I/C 5 questionnaire. *Mar. Chem.* **56**(1-2): 59-75. https://doi.org/10.1016/S0304-4203(96)00080-1, 1997.

Aminot, A. and Kérouel R.: *Dosage automatique des nutriments dans les eaux marines. Méthodes en flux continu*. Ed. Ifremer; 336 p. ISBN 2-84433-133-5, 2007.

Andersen, O. K., Goldman, J. C., Caron, D. A., and Dennett, M. R.: Nutrient cycling in a microflagellate food chain: III. Phosphorus dynamics. *Mar. Ecol. Prog. Ser.* **31**: 47-55, 1986.

Andersson, A., Brugel, S., Paczkowska, J., Rowe, O. F., Figueroa, D., Kratzer, S., and Legrand, C.: Influence of allochthonous dissolved organic matter on pelagic basal production in a northerly estuary. *Est. Coast. Shelf Sci.* **204**: 225-235. https://doi.org/10.1016/j.ecss.2018.02.032, 2018.

Andersson, A., Grinienė, E., Berglund, A. M. M., et al.: Microbial food web changes induced by terrestrial organic matter and elevated temperature in the coastal northern Baltic Sea. *Front. Mar. Sci.* **10**:1170054. https://doi.org/10.3389/fmars.2023.1170054, 2023.

Alpert, P., Ben-Gai, T., Baharad, A., *et al.*: The paradoxical increase of Mediterranean extreme daily rainfall in spite of decrease in total values, *Geophys. Res. Lett.* **29**(11). https://doi.org/10.1029/2001GL013554, 2002.

Ask, J., Karlsson, J., and Jansson, M.: Net ecosystem production in clear-water and brown-water lakes. *Glob. Biogeochem. Cyc.* **26**(1). https://doi.org/10.1029/2010GB003951, 2012.

Behrenfeld, M. J., Prasil, O., Babin, M., and Bruyant, F.: In search of a physiological basis for covariations in light limited and light saturated photosynthesis. *J. Phycol.* **40**(1): 4-25. https://doi.org/10.1046/j.1529-8817.2004.03083.x, 2004.

Blanchet, C. C., Arzel, C., Davranche, A., Kahilainen, K. K., Secondi, J., Taipale, S., Lindberg, H., Loehr, J., Manninen-Johansen, S., *et al.*: Ecology and extent of freshwater browning – What we know and what should be studied next in the context of global change. *Sci. Tot. Env.* **812**: 152420. https://doi.org/10.1016/j.scitotenv.2021.152420, 2022.

Brussaard, C. P. D.: Viral control of phytoplankton populations – a review. J. Euk. Microb. 51:125-138. https://doi.org/10.1111/j.1550-7408.2004.tb00537.x, 2004.

Carrit, D. E., and Carpenter, J. H.: Comparison and evaluation of currently employed modifications of the Winkler method for determining oxygen in seawater. A NASCO report. *J. Mar. Res.* **24**: 286-318, 1966.

https://doi.org/10.5194/egusphere-2023-2782
Preprint. Discussion started: 24 November 2023

Clayton, T. D., and Byrne, R. H.: Spectrophotometric seawater pH measurements: Total hydrogen ion concentration scale calibration of m-cresol purple and at-sea results. *Deep Sea Res. I: Oceanogr. Res. Papers* **40**(10): 2115–2129. https://doi.org/10.1016/0967-0637(93)90048-8, 1993.

Courboulès, J., Vidussi, F., Soulié, T., Mas, S., Pecqueur, D., and Mostajir, B. : Effects of experimental warming on small phytoplankton, bacteria and viruses in autumn in the Mediterranean coastal Thau lagoon. *Aquat. Ecol*. **55**:647-666. https://doi.org/10.1007/s10452-021-09852-7, 2021.

Courboulès, J., Vidussi, F., Soulié, T., Nikiforakis, E., Heydon, M., Mas, S., Joux, F., and Mostajir, B.: Effects of an experimental terrestrial runoff on the components of the plankton food web in a Mediterranean coastal lagoon. *Font. Mar. Sci.* **10**:1200757. https://doi.org/10.3389/fmars.2023.1200757, 2023.

Deininger, A., Faithfull, C. L., Lange, K., Bayer, T., Vidussi, F., and Liess, A.: Simulated terrestrial runoff triggered a phytoplankton succession and changed stoichiometry in coastal lagoon mesocosms. *Mar. Env. Res*. **119**:40-50. https://doi.org/10.1016/j.marenvres.2016.05.001, 2016.

Deininger, A., and Frigstad, H.: Reevaluating the role of organic matter sources for coastal eutrophication, oligotrophication, and ecosystem health. *Front. Mar. Sci*. **6**. https://doi.org/10.3389/fmars.2019.00210, 2019.

Deppeler, S., Petrou, K., Schulz, K. G., Westwood, K., Pearce, I., McKinlay, J., and Davidson, A.: Ocean acidification of a coastal Antarctic marine microbial community reveals a critical threshold for CO_2 tolerance in phytoplankton productivity. *Biogeosciences* **15**: 209-231. https://doi.org/10.5194/bg-15-209-2018, 2018.

Derolez, V., Soudant, D., Malet, N., Chiantella, C., Richard, M., Abadie, E., *et al*.: 2020. Two decades of oligotrophication: evidence for a phytoplankton community shift in the coastal lagoon of Thau (Mediterranean Sea, France). *Estuar. Coast. Shelf Sci*. **241**:106810. https://doi.org/10.1016/j.ecss.2020.106810, 2020.

Dickson, A. G.: Standard potential of the reaction: AgCl(s) + 1 $2H_2$(g) = Ag(s) + HCl (aq), and the standard acidity constant of the ion HSO_4^- in synthetic sea water from 273.15 to 318.15 K. *J. Chem. Thermodyn.* **22**(2): 113–127. https://doi.org/10.1016/0021-9614(90)90074-Z, 1990.

Dickson, A. G., Sabine, C. L., Christian, J. R., and North Pacific Marine Science Organization.: Guide to best practices for ocean CO_2 measurements. *North Pacific Marine Science Organization*. https://www.oceanbestpractices.net/handle/11329/249, 2007.

Ducrocq, V., Nuissier, O., Ricard, D., Lebeaupin, C., and Thouvenin, T.: A numerical study of three catastrophic precipitating events over southern France. II: Mesoscale triggering and stationary factors. *Q.J.R. Meteorol. Soc.* **134**:131-145. https://doi.org/10.1002/qj.199, 2008.

Falkowski, P. G., Laws, E. A., Barber, R. T., and Murray, J. W.: Phytoplankton and their role in primary, new and export production. In: Fasham, M. J. R. (Eds). *Ocean Biogeochemistry. Global Change – The IGBP Series* (closed). Springer, Berlin, Heidelberg. https://doi.org/10.1007/978-3-642-55844-3_5, 2003.

Falkowski, P.: Ocean science: the power of plankton. *Nature* **483**, S17–S20. https://doi.org/10.1038/483S17a, 2012.

Fouilland, E., Trottet, A., Bancon-Montigny, C., *et al*.: Impact of a river flash flood on microbial carbon and nitrogen production in a Mediterranean lagoon (Thau lagoon, France). *Est. Coast. Shelf Sci.* **113**:192-204. https://doi.org/10.1016/j.ecss.2012.08.004, 2012.

Giller, P. S., Hillebrand, H., Berninger, U.-G., Gessner, M. O., Hawkins, S., Inchausti, P., Inglis, C., Leslie, H., Malmqvist, B., *et al*.: Biodiversity effects on ecosystem functioning: emerging issues and their experimental test in aquatic environments. *Oikos* **104**:423-436. https://doi.org/10.1111/j.0030-1299.2004.13253.x, 2004.

Glibert, P. M.: Regional studies of daily, seasonal and size fraction variability in ammonium remineralization. *Mar. Biol*. **70**:209-222. https://doi.org/10.1007/BF00397687, 1982.

Halsey, K. H., Milligan, A. J., and Behrenfeld, M. J.: Physiological optimization underlies growth rate-independent chlorophyll-specific gross and net primary production. *Photosynth. Res*. **103**: 125-137. https://doi.org/10.1007/s11120-009-9526-z, 2010.

Hernández-Ayón, J. M., Belli, S. L., and Zirino, A.: pH, alkalinity and total CO_2 in coastal seawater by potentiometric titration with a difference derivative readout. *Analytica Chimica Acta* **394**(1): 101–108. https://doi.org/10.1016/S0003-2670(99)00207-X, 1999.

Hillebrand, H., Langenheder, S., Lebret, K., Lindström, E., Östman, Ö, and Striebel, M.: Decomposing multiple dimensions of stability in global change experiments. *Ecol. Lett.* **21**:21-30. https://doi.org/10.1111/ele.12867, 2018.

https://doi.org/10.5194/egusphere-2023-2782
Preprint. Discussion started: 24 November 2023

Holmes, R. M., Aminot, A., Kérouel, R., Hooker, B. A., and Peterson, B. J.: A simple and precise method for measuring ammonium in marine and freshwater ecosystems. *Can. J. Fish. Aq. Sci.* **56**(10): 1801-1808. https://doi.org/10.1139/f99-128, 1999.

Isles, P. D. F., Creed, I. F., Jonsson, A., and Bergström, A.-K.: Trade-offs between light and nutrient availability across gradients of dissolved organic carbon lead to spatially and temporally variable responses of lake phytoplankton biomass to browning. *Ecosystems* **24**: 1837-1852. https://doi.org/10.1007/s10021-021-00619-7, 2021.

Kiorboe, T., Andersen, K. P., and Dam, H. G.: Coagulation efficiency and aggregate formation in marine phytoplankton. *Mar. Biol*. **107**:235-245. https://doi.org/10.1007/BF01319822, 1990.

Klug, J. L.: Positive and negative effects of allochthonous dissolved organic matter and inorganic nutrients on phytoplankton growth. *Can. J. Fish. Aquat. Sci*. **59**(1): 85-95. https://doi.org/10.1139/f01-194, 2002.

La Jeunesse, I., Cirelli, C., Sellami, H., Aubin, D., Deidda, R., and Baghdadi, N. : Is the governance of the Thau coastal lagoon ready to face climate change impacts? *Ocean Coast. Manag*. **118**:234-246. https://doi.org/10.1016/j.ocecoaman.2015.05.014, 2015.

Landry, M. R., and Hassett, R. P.: Estimating the grazing impact of marine micro-zooplankton. *Mar. Biol*. **67**: 283-288. https://doi.org/10.1007/BF00397668, 1982.

Lee, K., Kim, T.-W., Byrne, R. H., Millero, F. J., Feely, R. A., and Liu, Y.-M.: The universal ratio of boron to chlorinity for the North Pacific and North Atlantic oceans. *Geochimica et Cosmochimica Acta* **74**(6): 1801–1811. https://doi.org/10.1016/J.GCA.2009.12.027, 2010.

Legendre, L., and Rassoulzadegan, F.: Plankton and nutrient dynamics in marine waters. *Ophelia* **41**(1): 153-172. https://doi.org/10.1080/00785236.1995.10422042, 1995.

Lewis, E., and Wallace, D. W. R.: Program Developed for CO_2 System Calculations, ORNL/CDIAC-105. Carbon Dioxide Information Analysis Center. Oak Ridge, TN: Oak Ridge National Laboratory. U.S, Department of Energy. https://doi.org/10.15485/1464255, 1998.

Liess, A., Rowe, O., Francoeur, S. N., *et al*.: Terrestrial runoff boosts phytoplankton in a Mediterranean coastal lagoon, but these effects do not propagate to higher trophic levels. *Hydrobiologia* **766**:275-291. https://doi.org/10.1007/s10750-015-2461-4, 2016.

Lopez-Urrutia, A., Martin, E. S., Harris, R. P., and Irigoien, X.: Scaling the metabolic balance of the oceans. *Proc. Natl. Acad. Sci. U. S. A.* **103**: 8739-8744. https://doi.org/10.1073/pnas.0601137103, 2006.

Lueker, T. J., Dickson, A. G., and Keeling, C. D.: Ocean pCO_2 calculated from dissolved inorganic carbon, alkalinity, and equations for K_1 and K_2: validation based on laboratory measurements of CO_2 in gas and seawater at equilibrium. *Mar. Chem*. **70**(1): 105-119. https://doi.org/10.1016/S0304-4203(00)00022-0, 2000.

Marie, D., Partensky, F., Jacquet, S., and Vaulot, D.: Enumeration and cell cycle analysis of natural populations of marine picoplankton by flow cytometry using the nucleic acid stain SYBR Green I. *Appl. Environ. Microbiol*. **63**:186-193. https://doi.org/10.1128/AEM.63.1.186-193.1997, 1997.

Meunier, C., Liess, A., Andersson, A., Brugel, S., Paczkowska, J., Rahman, H., Skoglund, B., and Rowe, O. F.: Allochthonous carbon is a major driver of the microbial food web – A mesocosm study simulating elevated terrestrial matter runoff. *Mar. Env. Res*. **129**:236-244, https://doi.org/10.1016/j.marenvres.2017.06.008, 2017.

Mostajir, B., Amblard, C., Buffan-Dubau, E., de Wit, R., Lensi, R., and Sime-Ngando, T.: Microbial food webs in aquatic and terrestrial ecosystems. In: Bertrand J-C., Caumette P., Lebaron P., Normand P., Sime-Ngando T. (Eds): *Environmental Microbiology: Fundamentals and Applications.* Springer. The Netherlands. Chapter **13**: 458-509, 2015.

Müller, O., Seuthe, L., Bratbak, G., and Paulsen, M. L.: Bacterial response to permafrost derived organic matter input in an Arctic fjord. *Front. Mar. Sci.* **5**. https://doi.org/10.3389/fmars.2018.00263, 2018.

Mustaffa, N., Kallajoki, L., Biederbick, J., Binder, F., Schlenker, A., and Striebel, M.: Coastal ocean darkening effects via terrigenous DOM addition on plankton: an indoor mesocosm experiment. *Front. Mar. Sci*. **7**. https://doi.org/10.3389/fmars.2020.547829, 2020.

https://doi.org/10.5194/egusphere-2023-2782
Preprint. Discussion started: 24 November 2023

Nixon, S. W.: Remineralization and nutrient cycling in coastal marine ecosystems. In: Neilson B. J., Cronin L. E. (eds) Estuaries and nutrients. Contemporary Issues in Science and Society. Humana Press. https://doi.org/10.1007/978-1-4612-5826-1_6, 1980.

Nunes, J. P., Seixas, J., Keizer, J. J., and Ferreira, A. J. D.: Sensitivity of runoff and soil erosion to climate change in two Mediterranean watersheds. Part I: model parameterization and evaluation. *Hydrol. Process* **23**, 1202e1211. https://doi.org/10.1002/hyp.7247, 2009.

Paczkowska, J., Brugel, S., Rowe, O., Lefébure, R., Brutemark, A., and Andersson, A.: Response of coastal phytoplankton to high inflows of terrestrial matter. *Front. Mar. Sci*. **7**. https://doi.org/10.3389/fmars.2020.00080, 2020.

Pecqueur, D., Vidussi, F., Fouilland, E., Le Floc'h, E., Mas, S., Roques, C., Salles, C., Tournoud, M.-G., and Mostajir, B.: Dynamics of microbial planktonic food web components during a river flash flood in a Mediterranean coastal lagoon. *Hydrobiologia* **673**:13-27. https://doi.org/10.1007/s10750-011-0745-x, 2011.

Pierrot, D. E., Lewis, D., and Wallace, W. R.: *MS Excel Program Developed for CO_2 System Calculations. ORNL/CDIAC-105a*. Oak Ridge, Tennessee: Carbon Dioxide Information Analysis Center, Oak Ridge National Laboratory, U.S. Department of Energy. https://doi.org/10.3334/CDIAC/otg.CO2SYS_XLS_CDIAC105a, 2006.

Plus, M., La Jeunesse, I., Bouraoui, F., Zaldivar, J.-M., Chapelle, A., and Lazure, P.: Modelling water discharges and nitrogen inputs into a Mediterranean lagoon: Impact on the primary production. *Ecol. Modell.* **193**(1-2): 69-89, https//doi.org/10.1016/j.ecolmodel.2005.07.037, 2006.

Robinson, C.: Heterotrophic bacterial respiration. In: Microbial Ecology of the Oceans, 2nd Edn, ed. D. L. Kirchman (Hoboken, NJ: Wiley). 299-334, 2008.

Sanchez, E., Gallardo, C., Gaertner, M. A., Arribas, A., Castro, M.: Future climate extreme events in the Mediterranean simulated by a regional climate model: a first approach. *Glob. Planet. Change* **44**, 163e180. https://doi.org/10.1016/j.gloplacha.2004.06.010, 2004.

Scharnweber, K., Peura, S., Attermeyer, K., *et al*.: Comprehensive analysis of chemical and biological problems associated with browning agents used in aquatic studies. *Limnol. Oceanogr. Methods* **19**: 818-835. https://doi.org/10.1002/lom3.10463, 2021.

Soria, J., Pérez, R., and Soria-Pepinya, X.: Mediterranean coastal lagoons review: Sites to visit before disappearance. *J. Mar. Sci. Eng*. **10**(3): 347. https://doi.org/10.3390/jmse10030347, 2022.

Soulié, T., Mas, S., Parin, D., Vidussi, F., and Mostajir, B. : A new method to estimate planktonic oxygen metabolism using high-frequency sensor measurements in mesocosm experiments and considering daytime and nighttime respirations. *Limnol. Oceanogr. Methods* **19**:303-316. https://doi.org/10.1002/lom3.10424, 2021.

Soulié, T., Vidussi, F., Mas, S., and Mostajir, B.: Functional stability of a coastal Mediterranean plankton community during an experimental marine heatwave. *Front. Mar. Sci*. **9**:831496. https://doi.org/10.3389/fmars.2022.831496, 2022a.

Soulié, T., Stibor, H., Mas, S., *et al*.: Brownification reduces oxygen gross primary production and community respiration and changes the phytoplankton community composition: an *in situ* mesocosm experiment with high-frequency sensor measurements in a North Atlantic Bay. *Limnol. Oceanogr*. **67**(4): 874-887. https://doi.org/10.1002/lno.12041, 2022b.

Soulié, T., Vidussi, F., Courboulès, J., Heydon, M., Mas, S., Voron, F., Cantoni, C., Joux, F., and Mostajir, B.: Dataset from a mesocosm experiment testing the effects of a terrestrial runoff on a Mediterranean plankton community. *SEANOE*. https://doi.org/10.17882/97260, 2023.

Staehr, P. A., Bade, D., de Bogert, M. C. V., Koch, G. R., Williamson, C., Hanson, P., *et al*.: Lake metabolism and the diel oxygen technique: state of the science. *Limnol. Oceanogr. Methods* **8**:628-644. https://doi.org/10.4319/lom.2010.8.0628, 2010.

Strandberg, U., Hiltunen, M., Creed, I. F., Arts, M. T., and Kankaala, P.: Browning-induced changes in trophic functioning of planktonic food webs in temperate and boreal lakes: insights from fatty acids. *Oecologia* **201**: 183-197. https://doi.org/10.1007/s00442-022-05301-w, 2023.

Strasser, R. J., Srivastava, A., and Tsimilli-Michael, M.: The fluorescence transient as a tool to characterize and screen photosynthetic samples. In: Yunus, M., Pathre, U., Mohanty, P. (Eds.). *Probing photosynthesis: Mechanisms, regulation and adaptation*. Taylor and Francis, UK, pp445-483, 2000.

Striebel, M., Kallajoki, L., Kunze, C., Wollschläger, J., Deininger, A., and Hillebrand, H.: Marine primary producers in a darker future: a meta-analysis of light effects on pelagic and benthic autotrophs. *Oikos* e09501. https://doi.org/10.1111/oik.09501, 2023.

https://doi.org/10.5194/egusphere-2023-2782
Preprint. Discussion started: 24 November 2023

Traving, S. J., Rowe, O., Jakobsen, N. M., Sorensen, H., Dinasquet, J., Stedmon, C. A., Andersson, A., and Riemann, L.: The effect of increased loads of dissolved organic matter on estuarine microbial community composition and function. *Front. Microb*. **8**. https://doi.org/10.3389/fmicb.2017.00351, 2017.

Trinh, D. A., Luu, T. N. M., Trinh, Q. H., *et al*.: Impact of terrestrial runoff on organic matter, trophic state, and phytoplankton in a tropical, upland reservoir. *Aquat. Sci*. **78**: 367-379. https://doi.org/10.1007/s00027-015-0439-y, 2016.

Trombetta, T., Vidussi, F., Mas, S., Parin, D., Simier, M, and Mostajir, B.: Water temperature drives phytoplankton blooms in coastal waters. *Plos ONE* **14**(4): e0214933. https://doi.org/10.1371/journal.pone.0214933, 2019.

Vadstein, O., Brekke, O., Andersen, T., and Olsen, Y.: Estimation of phosphorus release rates from natural zooplankton communities feeding on planktonic algae and bacteria. *Limnol. Oceanogr*. **40**(2): 250-262. https://doi.org/10.4319/lo.1995.40.2.0250, 1995.

Zapata, M., Rodriguez, F., and Garrido, J. L.: Separation of chlorophylls and carotenoids from marine phytoplankton: a new HPLC method using a reversed phase C8 column and pyridine-containing mobile phases. Mar. Ecol. Prog. Ser. 195: 29-45, https://doi.org/10.3354/meps195029, 2000.